energies

MDPI

Article

A New Dynamic Injection System of Urea-Water Solution for a Vehicular Select Catalyst Reduction System

Long Li, Wei Lin and Youtong Zhang *

School of Mechanical Engineering, Beijing Institute of Technology, Beijing 100081, China; voyage_lee@163.com (L.L.); lin_wei_sky@163.com (W.L.)

* Correspondence: youtong@bit.edu.cn; Tel.: +86-10-6891-5013

Academic Editor: Evangelos G. Giakoumis

Received: 28 September 2016; Accepted: 9 December 2016; Published: 23 December 2016

Abstract: Since the Euro-III standard was adopted, the main methods to inhibit NO_x production in diesel engines are exhaust gas recirculation (EGR) and select catalyst reduction (SCR). On these methods SCR offers great fuel economy, so it has received wide attention. However, there also exists a trade-off law between NO_x conversion efficiency and NH_3 slip under dynamic conditions. To inhibit NH_3 slip with high NO_x conversion efficiency, a dynamic control method for a urea water solution (UWS) injection was investigated. The variation phenomena of SCR conversion efficiency with respect to the cross-sensitivity characteristics of the NO_x sensor to NH_3 have been thoroughly analyzed. The methodology of "uncertain conversion efficiency curve tangent analysis" has been applied to estimate the concentration of the slipped NH_3. The correction factor "φ" of UWS injection is obtained by a comparative calculation of the NO_x conversion ability and subsequent NH_3 slip. It also includes methods of flow compensation and flow reduction. The proposed control method has been authenticated under dynamic conditions. In low frequency dynamic experiments, this control method has accurately justified the NH_3 slip process and inhibits the NH_3 emission to a lower level thereby improving the conversion efficiency to a value closer to the target value. The results of European transient cycle (ETC) experiments indicate that NH_3 emissions are reduced by 90.8% and the emission level of NO_x is close to the Euro-V standard.

Keywords: select catalyst reduction (SCR); urea water solution (UWS); NH_3 slip; dynamic correction

1. Introduction

Direct injection diesel engines are preferred for their superior economy, power and emissions. Due to the high combustion temperature of the diesel engine, the nitrogen in the air is easily oxidized by oxygen and produces a large amount of NO_x which have a significant pollution impact on the environment. Therefore, NO_x emissions should be controlled. High pressure fuel injection and turbocharging technology have been used to change the ratio of particulate matter (PM) and NO_x by regulating the fuel injection strategy. From the Euro-II to the Euro-III phase, the high injection pressure (high common rail fuel injection) system has been used to optimize in-cylinder combustion and regulate the ratio of PM and NO_x to reach the emission goals. From the Euro-III to the Euro-IV phase, the main problem is how to significantly reduce PM and NO_x emissions. There are two methods at present: one is to use exhaust gas recirculation (EGR) to reduce in-cylinder NO_x, and out of the cylinder, with diesel particulate filter(DPF) to filter PM; the other method is to use select catalyst reduction (SCR) to eliminate NO_x and PM. In small diesel engines, the SCR system is limited by the exhaust gas temperature, so EGR + DPF technology is used as the main method to solve the emission problem. The exhaust temperature of medium and heavy diesel engines is high. At high exhaust temperatures, diesel engines with SCR + high-pressure common rail (HCR) technology are more economical than diesel engines with EGR + DPF technology, so SCR is more widely used in medium and heavy duty diesel engines. From the Euro-IV to the Euro-V phase, how to further reduce NO_x has become the key problem. The main method is to optimize the SCR system to enhance the NO_x conversion efficiency and reduce the NH_3 leakage [1–6].

At present, almost 99% of diesel vehicles work under dynamic operating conditions and thus their NO_x emissions are also a dynamic process. Based on this condition, excellent dynamic performance is an essential characteristic of the SCR system. SCR control strategies mainly focus on optimizing the urea water solution (UWS) injection rate algorithms and NH_3 slip inhibition. However, there is a trade-off law between NO_x conversion efficiency and NH_3 slip under dynamic conditions. When the actual injection rate is lower than the theoretical one, the NO_x can't be completely reduced. When the actual injection rate is higher than the theoretical value, NH_3 can't be completely oxidized and thus generates secondary pollution [7–9]. Furthermore, NH_3 storage and catalyst release make the NH_3 slip inhibition more difficult.

Some researchers believe that an oxidation processor installed at the end of the exhaust pipe may inhibit NH_3 slip [10]. Nova and Tronconi [11] added an Ammonia Slip Catalyst (ASC) to the exhaust pipe downstream of the SCR system and completed some investigations by experiment and simulation. The results showed that the studied ASC could efficiently clean up the slipped NH_3. Shrestha et al. [12] did some experiments and simulation research on multi-functional wash coated monolith catalysts. They compared the catalysts for a range of temperatures, space velocities, and feed compositions in the presence of H_2O and CO_2. Based on the data acquired from the experiments, a dynamic model of the NH_3 oxidation process was established.

Some researchers supposed that it is necessary to investigate the processes of NH_3 storage, release and reduction reaction as well as the SCR catalyst [13,14]. Rauch et al. [15] monitored the ammonia loading of a vanadia-based SCR catalyst by a microwave-based method. Their experimental results showed that the method can be applied to different temperatures. It was also possible to determine the storage of ammonia from the ammonia-to-NO_x feed ratio. Zhang and Wang [16] focused on the simultaneous estimation of ammonia coverage ratios and input. They configured a three-state nonlinear model with the high-gain observer method by assuming the states of the SCR system are homogenous inside and the SCR cell was a continuous stirred tank reactor. The NO_x sensor was cross-sensitive to the NH_3 concentration, and the NO_x sensor reading was corrected by precise NH_3 sensor measurements. The simulation results showed that the designed observer worked well.

NO_x sensors are used to measure the NO_x concentration downstream from the SCR system and feed it back to the SCR controller. However, research results have showed that NO_x sensors have an enhanced cross sensitivity to NH_3 [17–19]. According to the structural characteristics of NO_x sensors, the NH_3 inside the sensor is easily oxidized to NO_x. There are mainly three chemical reactions in this process, as described in Equations (1)–(3) [20–23]:

$$2NH_3 + 2O_2 \rightarrow N_2O + 3H_2O \quad (1)$$

$$2NH_3 + 2.5O_2 \rightarrow 2NO \ + \ 3H_2O \quad (2)$$

$$2NH_3 + 3.5O_2 \rightarrow 2NO_2 + 3H_2O \quad (3)$$

Wang [24] believed that the main factor is temperature, which may affect the three chemical reactions. The cross sensitivity factor of the NO_x sensor is changed as the temperature changes. Experiments proved that this factor was between 0.5 and 2 for a range of diesel engine exhaust temperatures.

This paper focuses on the trade-off law between NO_x conversion efficiency and NH_3 slip by using a presented method of "uncertain conversion efficiency curve tangent analysis" based on the NH_3 cross sensitivity characteristics of the NO_x sensor. The degree of NH_3 slip will be obtained from the calculation of the parameters which may affect the shape and locations of this tangent. Subsequently, the UWS injection correction factor "φ" will be calculated with the dynamic flow compensation and flow reduction. Finally the accuracy of the UWS correction model and the effectiveness of NH_3 slip inhibition will be verified under low-frequency and high-frequency (ETC cycle) dynamic working conditions.

2. Correction Strategy Mathematical Analysis

For the SCR system control strategy, the corrected UWS injection rate is calculated by Equation (4):

$$q_{\text{uws,Act}} = (1 + \varphi) \times q_{\text{uws,Bas}} \tag{4}$$

where $q_{\text{UWS,Act}}$ is the real-time UWS injection rate after correction, $q_{\text{UWS,Bas}}$ is the basic UWS injection rate before correction and φ is the correction factor of the UWS injection rate. The Simulink model of the correction strategy is shown in Figure 1.

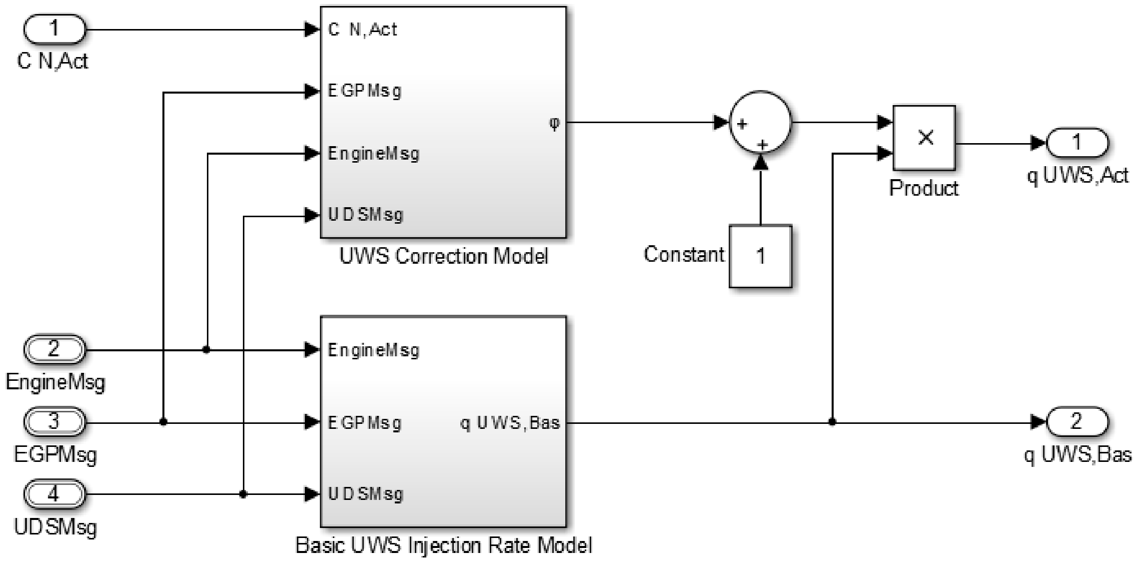

Figure 1. The correction strategy model. UWS: urea water solution.

The model consists of two sub-models. The "Basic UWS Injection Rate Model" sub-model collects three pieces of data: (1) engine operating data *EngineMsg*, which include speed, torque, original emissions, etc.; (2) exhaust gas processor data *EGPMsg*, which include exhaust temperature before and after the catalyst, gas flow, etc.; (3) injection system data *UDSMsg*. These data are combined to calculate $q_{\text{UWS,Bas}}$.

The "UWS Correction Model" sub-model collects four sets of data: (1) engine operating data; (2) waste gas treatment data; (3) urea injection system data; and (4) NO_x sensor data. These data are processed in the module to obtain the UWS injection rate correction factor φ. The $q_{\text{UWS,Act}}$ is calculated using the factor φ and $q_{\text{UWS,Bas}}$.

The change rule of $q_{\text{UWS,Act}}$ can be obtained from Equation (5):

$$a_{\text{UWS,Act}} = \frac{\partial q_{\text{uws,Act}}}{\partial t} = q_{\text{uws,Bas}} \frac{\partial \varphi}{\partial t} + (1 + \varphi) \frac{\partial q_{\text{uws,Bas}}}{\partial t} \tag{5}$$

where $a_{\text{UWS,Act}}$ is the acceleration of $q_{\text{UWS,Act}}$, and t is the time.

The "φ" (the initial value is "0") is the key factor to correct the UWS injection and keep the SCR system at a low NH_3 slip level with a high conversion efficiency. The UWS correction model is shown in Figure 2.

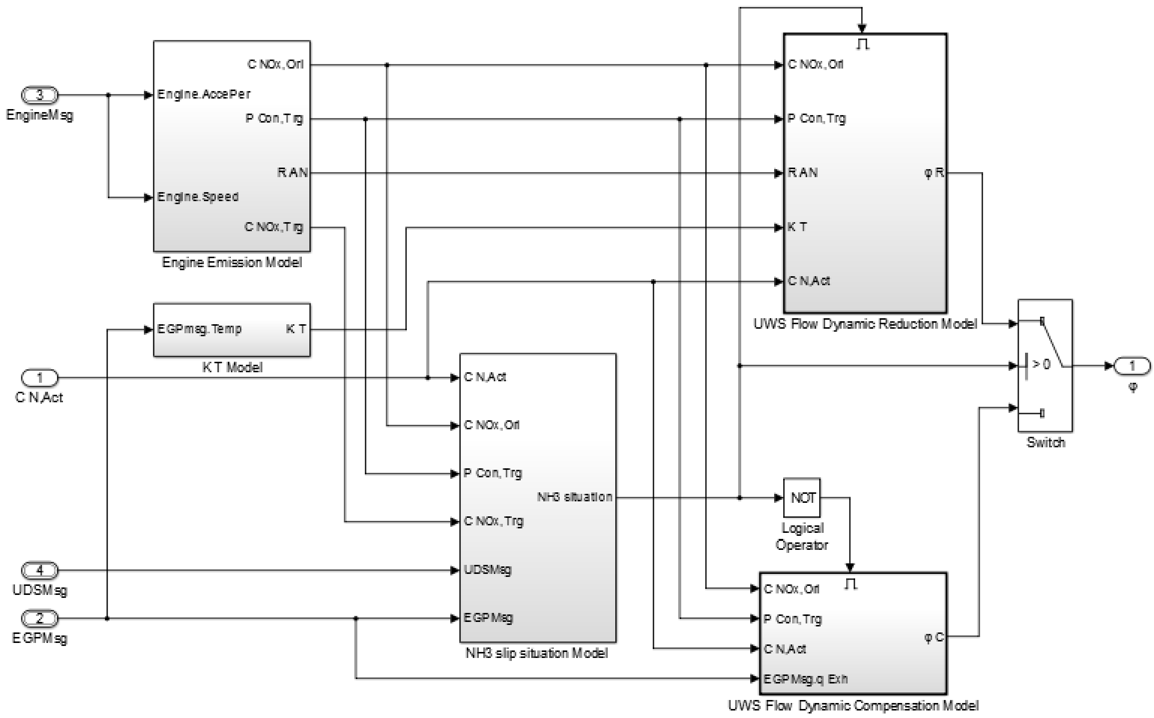

Figure 2. The UWS correction model.

The UWS correction model consists of five sub-models:

The "K_T Model" sub-model calculates the real-time NH_3 sensitivity factor of the sensor based on the exhaust gas temperature near the NO_x sensor. The NO_x emission was measured by a NO_x sensor under dynamic conditions. The surrounding NH_3 may be converted into NO_x easily in the NO_x sensor. Therefore, the values of NH_3 and NO_x at the same time will be influenced by the data which is measured by the NO_x sensor, as given by Equation (6):

$$C_{\mathrm{N,Act}} = C_{\mathrm{NO}_x\mathrm{,Act}} + K_{\mathrm{T}} C_{\mathrm{NH}_3\mathrm{,Act}} \quad (6)$$

where $C_{\mathrm{N,Act}}$ is the NO_x concentration measured by the NO_x sensor. $C_{\mathrm{NO}_x\mathrm{,Act}}$ is the actual NO_x concentration at the testing position. K_{T} is the NH_3 cross sensitivity factor of the NO_x sensor which could be obtained from the K_{T} map and $C_{\mathrm{NH}_3\mathrm{,Act}}$ is the actual NH_3 concentration at the testing position.

The "Engine Emission Model" sub-model is used to calculate the original engine NO_x emissions, the target conversion efficiency, the ammonia-nitrogen ratio and the target NO_x emission concentration which would support service for the other models as shown in Figure 3. For example the targeted conversion efficiency could be calculated using Equation (7):

$$C_{\mathrm{NO}_x\mathrm{,Trg}} = C_{\mathrm{NO}_x\mathrm{,Ori}} \cdot P_{\mathrm{Con,Trg}} \quad (7)$$

where $P_{\mathrm{Con,Trg}}$ is the target conversion efficiency (the highest value without NH_3 slip) which can be obtained from the engine emission map, $C_{\mathrm{NO}_x\mathrm{,Ori}}$ is the original NO_x concentration of the engine before after treatment and can be obtained by inserting the value calculation of the steady map and $C_{\mathrm{NO}_x\mathrm{,Trg}}$ is the target NO_x concentration.

The "NH_3 Slip Situation Model" sub-model is based on the output of the first two models to determine the current NH_3 leak situation; more details can be seen in Section 2.1. The "UWS Flow Dynamic Reduction Model" sub-model is triggered when an NH_3 leak occurs. When there is no NH_3 leakage, it is necessary to consider whether there is little UWS injection and trigger the "UWS Flow Dynamic Compensation Model".

The "UWS Flow Dynamic Compensation Model" and "UWS Flow Dynamic Reduction Model" sub-models are used to calculate the correction factor and compensation factor of the UWS injection rate, respectively (see Sections 2.2 and 2.3 for more details).

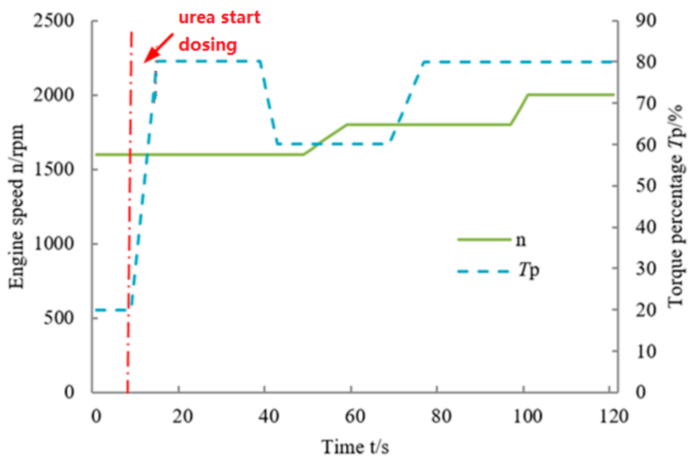

Figure 3. Low frequency dynamic process.

2.1. NH_3 Slip Situation Analysis

In order to justify and analyze the real-time NH_3 slip situation of the engine, a method called "uncertain conversion efficiency curve tangent analysis" is presented. From the real-time measured value $C_{N,Act}$, the uncertain conversion efficiency $P_{Con,Fuz}$ can be calculated using Equation (8). The absolute conversion efficiency $P_{Con,Abs}$ can be obtained from the calculated valve $C_{NO_x,Act}$ by Equation (9):

$$P_{Con,Fuz} = \frac{C_{NO_x,Ori} - C_{N,Act}}{C_{NO_x,Ori}} = 1 - \frac{C_{N,Act}}{C_{NO_x,Ori}} \quad (8)$$

$$P_{Con,Abs} = \frac{C_{NO_x,Ori} - C_{NO_x,Act}}{C_{NO_x,Ori}} = \frac{\left[C_{NO_x,Ori} - \left(C_{N,Act} - K_T C_{NH_3,Act}\right)\right]}{C_{NO_x,Ori}} = P_{Con,Fuz} + \frac{K_T C_{NH_3,Act}}{C_{NO_x,Ori}} \quad (9)$$

According to the results of Equations (8) and (9), the relative conversion efficiency can be calculated with Equation (10):

$$P_{Con,Rel} = P_{Con,Abs} - P_{Con,Trg} = P_{Con,Fuz} + \frac{K_T C_{NH_3,Act}}{C_{NO_x,Ori}} - P_{Con,Trg} \quad (10)$$

The change rules of $P_{Con,Fuz}$, $P_{Con,Abs}$, and $P_{Con,Rel}$ can be obtained from Equations (11)–(13):

$$v_{Con,Fuz} = \dot{P}_{Con,Fuz} = -\frac{\partial\left(\frac{C_{N,Act}}{C_{NO_x,Ori}}\right)}{\partial t} \quad (11)$$

$$v_{Con,Abs} = \dot{P}_{Con,Abs} = \frac{\partial P_{Con,Fuz} + \partial\left(\frac{K_T C_{NH_3,Act}}{C_{NO_x,Ori}}\right)}{\partial t} \quad (12)$$

$$v_{Con,Rel} = v_{Con,Abs} - v_{Con,Trg} = \frac{\partial P_{Con,Fuz} + \partial\left(\frac{K_T C_{NH_3,Act}}{C_{NO_x,Ori}}\right) - \partial P_{Con,Trg}}{\partial t} \quad (13)$$

where $v_{Con,Abs}$, $v_{Con,Rel}$, and $v_{Con,Fuz}$ are their velocities. There are several kinds of NH_3 slip situations, as follows:

(1) $P_{Con,Fuz} > P_{Con,Trg}$

For the original map of $P_{Con,Trg}$ obtained from the engine calibration experiments, from the theoretically point of view, with the $P_{Con,Fuz} \leq P_{Con,Trg}$ under any circumstances. In the actual conditions when the engine calibration points are not enough, engine working instability or sensor testing errors might occur and lead to an abnormal circumstance (like $P_{Con,Fuz} > P_{Con,Trg}$). For such an instance the NH_3 slip is assumed to be zero, thus the UWS need not be corrected.

(2) $0 \leq P_{Con,Fuz} \leq P_{Con,Trg}$, and $\tan\theta < 0$ ($v_{Con,Fuz} < 0$)

In this case, the uncertain conversion efficiency is lower than its target and stays away from the target value gradually. According to Equation (8), $P_{Con,Fuz}$ becomes smaller due to the increase of the $C_{N,Act}$. The enlargement of the $C_{N,Act}$ may be caused by the following two cases:

- The first case is that the excessively injected UWS caused an acceleration of the process and subsequently an increasing NH_3 slip due unreacted ammonia.
- The second case is that insufficient UWS may cause a slowing the process and lead to a growing amount of NO_x remaining unreduced due to unavailability of reactant.

Therefore, it may be concluded that with the condition $a_{UWS,Act} \leq 0$ and $P_{Con,Abs} \leq P_{Con,Trg}$, there is no NH_3 slip, thus UWS compensation could be continued. When $a_{UWS,Act} > 0$ and $P_{Con,Abs} = P_{Con,Trg}$, NH_3 slip is severely increased, thus UWS injection should be reduced.

(3) $0 \leq P_{Con,Fuz} \leq P_{Con,Trg}$, and $\tan\theta \geq 0$ ($v_{Con,Fuz} \geq 0$)

In this case, the uncertain conversion efficiency is lower than its target and becomes close to the target value gradually. In this case it can be concluded that when $a_{UWS,Act} > 0$ and $P_{Con,Abs} \leq P_{Con,Trg}$, there is no NH_3 slip like the previous cases, thus UWS compensation should be continued. With the condition $a_{UWS,Act} \leq 0$ and $P_{Con,Abs} \geq P_{Con,Trg}$, UWS injection should be reduced as NH_3 slip is going to increase.

(4) $P_{Con,Fuz} < 0$

This particular case emerges on ruling out the test error and the engine calibration map error, thus under these circumstances $C_{NO_x,Act} \leq C_{NO_x,Ori}$ (theoretically), whereas, $C_{N,Act} > C_{NO_x,Ori}$ ($P_{Con,Fuz} < 0$), $C_{NH_3,Act} > 0$ as shown in Equation (7). This case indicates a seriously high level of NH_3 slip therefore UWS injection must be stopped immediately.

2.2. Urea Water Solution Flow Dynamic Compensation

There was no NH_3 slip during the process of the UWS dynamic compensation. Therefore:

$$\begin{cases} C_{NH_3,Act} \equiv 0 \\ C_{NO_x,Act} \equiv C_{N,Act} \end{cases} \tag{14}$$

It is indicated that the actual amount of injected UWS (including the NH_3 released from the catalyst) was less than the demand of SCR reaction. The condition is $0 \leq P_{Con,Abs} \leq P_{Con,Trg}$ and zero NH_3 slip. Therefore, the correction factor φ can be calculated using Equation (15):

$$\varphi \equiv \frac{\Delta \dot{Q}_{NO_x,Red}}{\dot{Q}_{NO_x,ActRed}} \tag{15}$$

where $Q_{NO_x,Red}$ (NO_x conversion potential) is the difference between the target value and actual value of the total reduced NO_x in a period as shown by Equation (16) and $Q_{NO_x,AcRed}$ is the actual value of the total reduced NO_x in a specific period given by Equation (17):

$$\begin{aligned}\Delta Q_{NO_x,Re} &= \int C_{NO_x,Ori} P_{Con,Trg} q_{Exh} dt - \int (C_{NO_x,Ori} - C_{NO_x,Act}) q_{Exh} dt \\ &= \int \left[C_{N,Act} - C_{NO_x,Ori}\left(1 - P_{Con,Trg}\right)\right] q_{Exh} dt\end{aligned} \quad (16)$$

$$Q_{NO_x,ActRe} = \int (C_{NO_x,Ori} - C_{NO_x,Act}) q_{Exh} dt = \int (C_{NO_x,Ori} - C_{NO_x,N}) q_{Exh} dt \quad (17)$$

$$\varphi = \frac{\partial \Delta Q_{NO_x,Red}/\partial t}{\partial Q_{NO_x,ActRed}/\partial t} = \frac{\left[C_{N,Act} - C_{NO_x,Ori}\left(1 - P_{Con,Trg}\right)\right] q_{Exh}}{(C_{NO_x,Ori} - C_{N,Act}) q_{Exh}} = \frac{C_{NO_x,Ori} P_{Con,Trg}}{(C_{NO_x,Ori} - C_{N,Act})} - 1 \quad (18)$$

$$C_{N,Act} \leq C_{NO_x,Ori} \quad (19)$$

For the control method, the calculation of UWS injection rate and its acceleration may be accomplished with Equation (20) or Equation (21):

$$\begin{cases} q_{uws,Act} = \frac{C_{NO_x,Ori} P_{Con,Trg}}{(C_{NO_x,Ori} - C_{NO_x,N})} q_{uws,Bas} \\ a_{uws,Act} = q_{uws,Bas} \frac{\partial\left(\frac{C_{NO_x,Ori} P_{Con,Trg}}{C_{NO_x,Ori} - C_{N,Act}}\right)}{\partial t} + \\ \left(\frac{C_{NO_x,Ori} P_{Con,Trg}}{C_{NO_x,Ori} - C_{N,Act}}\right) \frac{\partial q_{uws,Bas}}{\partial t} \\ C_{N,Act} \leq C_{NO_x,Ori} \end{cases} \quad (20)$$

$$\begin{cases} q_{uws,Act} = 0 \\ a_{uws,Act} = 0 \\ C_{N,Act} \leq C_{NO_x,Ori} \end{cases} \quad (21)$$

where NH_3 slip is assumed to be zero.

The value of NO_x emission in this process may be obtained with:

$$\begin{cases} Q_{NO_x} = \int C_{N,Act} q_{Exh} dt \\ Q_{NH_3} \equiv 0 \end{cases} \quad (22)$$

2.3. Urea Water Solution Flow Dynamic Reduction

During the UWS dynamic process, reduction is the response of increasing NH_3 slip. Therefore:

$$\begin{cases} C_{NH_3,Act} \neq 0 \\ C_{NO_x,Act} + K_T \cdot C_{NH_3,Act} = C_{N,Act} \end{cases} \quad (23)$$

The case of $0 \leq P_{Con,Abs} \leq P_{Con,Trg}$ and presence of evident NH_3 slip shows that the actual amount of injected UWS (including the NH_3 released from the catalyst) is much more than the demand of the SCR reaction. This current situation indicates that the SCR reaction is saturated as shown by Equation (24):

$$C_{NO_x,Act} = C_{NO_x,Ori}\left(1 - P_{Con,Trg}\right) \quad (24)$$

According to Equation (7):

$$C_{NH_3,Act} = \frac{C_{N,Act} - C_{NO_x,Ori}\left(1 - P_{Con,Trg}\right)}{K_T} \quad (25)$$

The correction factor φ can be calculated as Equation (26):

$$\varphi = -\frac{\dot{Q}_{NH_3}}{R_{AN}\left(\dot{Q}_{NO_x,TrgRed} + \frac{Q_{NH_3}}{R_{AN}}\right)} = -\frac{\dot{Q}_{NH_3}}{\left(R_{AN}\dot{Q}_{NO_x,TrgRed} + Q_{NH_3}\right)} \tag{26}$$

where Q_{NH3} is the total NH_3 emission amount in a specific period of time given by Equation (27), $Q_{NOx,TrgRed}$ is the total reduced NO_x with target conversion efficiency of Equation (28) and R_{AN} is the ammonia nitrogen ratio constant set in the SCR system control strategy:

$$Q_{NH_3} = \int C_{NH_3,Act} q_{Exh} dt = \int \left[\frac{C_{N,Act} - C_{NO_x,Ori}\left(1 - P_{Con,Trg}\right)}{K_T}\right] q_{Exh} dt \tag{27}$$

$$\begin{aligned} \varphi &= -\frac{\partial Q_{NH_3}/\partial t}{\partial\left(R_{AN} Q_{NO_x,TrgRed} + Q_{NH_3}\right)/\partial t} \\ &= \frac{\left[C_{NO_x,Ori}\left(1-P_{Con,Trg}\right) - C_{N,Act}\right] q_{Exh}}{K_T\left(R_{AN} P_{Con,Trg} C_{NO_x,Ori} - \frac{C_{NO_x,Ori}\left(1-P_{Con,Trg}\right) - C_{N,Act}}{K_T}\right) q_{Exh}} \\ &= \frac{C_{NO_x,Ori}\left(1-P_{Con,Trg}\right) - C_{N,Act}}{K_T R_{AN} P_{Con,Trg} C_{NO_x,Ori} - C_{NO_x,Ori}\left(1-P_{Con,Trg}\right) + C_{N,Act}} \end{aligned} \tag{28}$$

Due to $q_{UWS,Act} \geq 0$ and $1 + \varphi \geq 0$:

$$C_{N,Act} \geq C_{NO_x,Ori} - (1 + K_T R_{AN}) P_{Con,Trg} C_{NO_x,Ori} \tag{29}$$

In the presence of NH_3 Slip, the control method may be applied to calculate the UWS injection rate and its acceleration is given by Equation (30) or Equation (31):

$$\begin{cases} q_{uws,Act} = \left(1 - \frac{1}{K_T R_{AN}} + \frac{C_{NO_x,Ori} - C_{N,Act}}{K_T R_{AN} P_{Con,Trg} C_{NO_x,Ori}}\right) q_{uws,Bas} \\ a_{uws,Act} = q_{uws,Bas} \frac{\partial\left(\frac{C_{NO_x,Ori} - C_{N,Act}}{R_{AN} P_{Con,Trg} C_{NO_x,Ori}} - \frac{1}{K_T R_{AN}}\right)}{\partial t} + \\ \left(1 - \frac{1}{K_T R_{AN}} + \frac{C_{NO_x,Ori} - C_{N,Act}}{K_T R_{AN} P_{Con,Trg} C_{NO_x,Ori}}\right) \frac{\partial q_{uws,Bas}}{\partial t} \\ C_{N,Act} \geq C_{NO_x,Ori} - (1 + K_T R_{AN}) P_{Con,Trg} C_{NO_x,Ori} \end{cases} \tag{30}$$

$$\begin{cases} q_{uws,Act} = 0 \\ a_{uws,Act} = 0 \\ C_{N,Act} \geq C_{NO_x,Ori} - (1 + K_T R_{AN}) P_{Con,Trg} C_{NO_x,Ori} \end{cases} \tag{31}$$

The amount of NO_x emission and NH_3 emission in this process could be determined by:

$$\begin{cases} Q_{NO_x} = \int C_{N,Act} q_{Exh} dt = \int C_{NO_x,Ori}\left(1 - P_{Con,Trg}\right) q_{Exh} dt \\ Q_{NH_3} = \int \left[C_{N,Act} - C_{NO_x,Ori}\left(1 - P_{Con,Trg}\right)\right] q_{Exh} dt \end{cases} \tag{32}$$

2.4. Special Case

For the special case of $P_{Con,Abs} > P_{Con,Trg}$, the actual value is more than the target value of the system conversion efficiency and NH_3 slip is assumed to be zero, as can be seen Equation (33):

$$\begin{cases} C_{NH_3,Act} \equiv 0 \\ C_{NO_x,Act} \equiv C_{N,Act} \end{cases} \tag{33}$$

The UWS injection rate doesn't require any dynamic adjustment thus $\varphi \equiv 0$. Therefore, it can be described with Equation (34) as follows:

$$\begin{cases} q_{\text{uws,Act}} = q_{\text{uws,Bas}} \\ a_{\text{uws,Act}} = \frac{\partial q_{\text{uws,Bas}}}{\partial t} \end{cases} \tag{34}$$

The amount of NO_x emission and NH_3 emission in this process are:

$$\begin{cases} Q_{NO_x} = \int C_{\text{N,Act}} q_{\text{Exh}} \text{d}t \\ Q_{NH_3} \equiv 0 \end{cases} \tag{35}$$

While in another special case where $P_{\text{Con,Fuz}} < 0$ indicates that NH_3 slip is very high. Thus UWS injection must be stopped immediately. Now $\varphi \equiv 0$, and:

$$\begin{cases} q_{\text{uws,Act}} = 0 \\ a_{\text{uws,Act}} = 0 \end{cases} \tag{36}$$

The amount of NO_x emission and NH_3 emission in this case can be described as follows:

$$\begin{cases} Q_{NO_x} = \int C_{\text{N,Act}} q_{\text{Exh}} \text{d}t = \int C_{NO_x,\text{Ori}} (1 - P_{\text{Con,Trg}}) q_{\text{Exh}} \text{d}t \\ Q_{NH_3} = \int [C_{\text{N,Act}} - C_{NO_x,\text{Ori}} (1 - P_{\text{Con,Trg}})] q_{\text{Exh}} \text{d}t \end{cases} \tag{37}$$

3. Experiments and Result Analysis

The low-frequency dynamic working conditions of the engine are reproduced as shown in Figure 1. The detailed dynamic process is shown in Figure 3. The related parameters of the SCR system are changed in a slower manner for this process by an explicit analysis of their relationships and interaction factors. Changes of NO_x emission and NH_3 slip are compared before and after the UWS dynamic correction. The ETC cycle was adopted for the high-frequency dynamic process for further verification of the UWS control method performance. The engine experiment platform is shown in Figure 4.

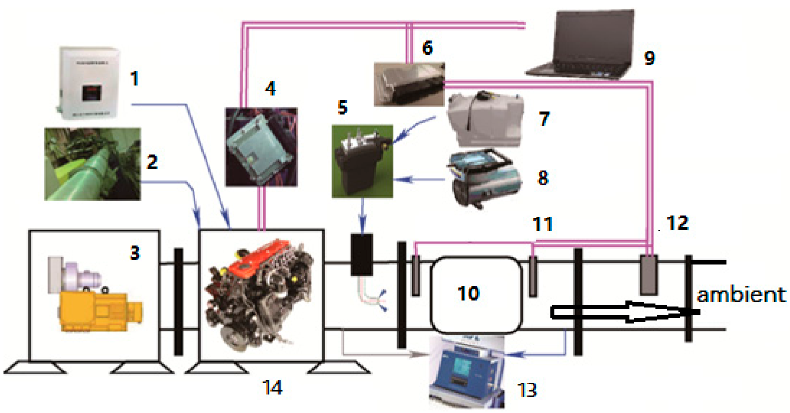

Figure 4. Engine experiment platform block diagram. 1: Fuel consumption; 2: Air flowmeter; 3: Dynamometer; 4: Electronic control unit (ECU); 5: Unified diagnostic services (UDS); 6: SCR control unit (SCU); 7: UWS tank; 8: Air pump; 9: Monitor; 10: Exterior gateway protocol (EGP); 11: Temperature sensor; 12: NO_x sensor; 13: Emissions analyzer; and 14: Diesel engine.

The specifications of main equipment in the engine experiment platform are listed in Table 1.

Table 1. Specifications of main equipment.

Name	Type	Manufacturer	Location	Remark
Diesel engine	ISDe270 40	DCEC	Xiangfan, China	L6
Dynamometer	GWD300	POWERLINK	Changsha, China	Eddy current style
Fuel consumption	FC2210	POWERLINK	Changsha, China	Quality style
Air flow meter	ToCeil	Shanghai ToCeil Engine Testing Equipment	Shanghai, China	Hot film style
Emissions analyzer	SESAM4.0	AVL	Graz, Austria	Fourier transform infrared spectroscopy

The heavy duty diesel engine parameters used in the experiment are given in Table 2.

Table 2. Parameters of ISDe270 40 diesel engine.

Cylinder Number	Bore/Stroke	Capacity	Compression Ratio	Rated Power/Speed	Max Torque	Fuel Supply Type
-	mm/mm	L	-	kW/rpm	Nm/rpm	-
L6	107/124	6.7	17.3:1	198/2500	970/1400	high pressure common rail

3.1. Mathematical Model Validation

As shown in Figure 5 (in this paper, A indicates the values after correction, B indicates the values before correction, T indicates the values obtained from equipment testing, C indicates the values obtained from calculation and M indicates the values obtained from the maps). The UWS injection was started at the 6th second. It can be seen in Figure 5 that the $C_{N,Act}$ curve declined gradually in the first 30 s, became stable at a very low level in the second 30 s, and two noticeable humps can be observed in the last 60 s. Considering the NH_3 cross sensitivity of the NO_x sensor, it could be initially assumed that the conversion efficiency was low in the first 30 s as the UWS injection was not sufficient. The NH_3 slip increased significantly in the position of the two humps with the severely overloaded UWS injection. The UWS correction under dynamic conditions is critical for improving SCR conversion efficiency and NH_3 slip inhibition.

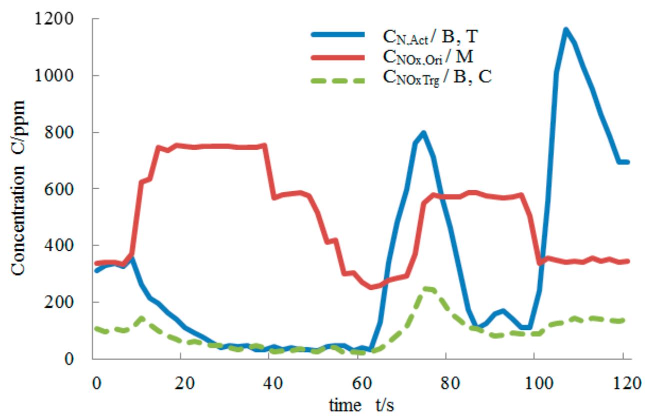

Figure 5. NO_x emissions in dynamic conditions before the correction.

The change rules of the four kinds of conversion efficiency which have been discussed in Section 2.1 are shown in Figure 6.

(1) In the beginning, $P_{Con,Abs}$ was less than the target valve $P_{Con,Trg}$. However, these two values are the same as that after the 30th second.
(2) $P_{Con,Fuz}$ and $P_{Con,Abs}$ remain the same as that before the 60th second. Then, two serious sinks appeared in the $P_{Con,Fuz}$ curve.
(3) After the beginning of UWS injection, $P_{Con,Rel}$ was stable near a 0 value between the 20th and 60th second and fluctuated in a range of ±30% between the 60th and 120th second.

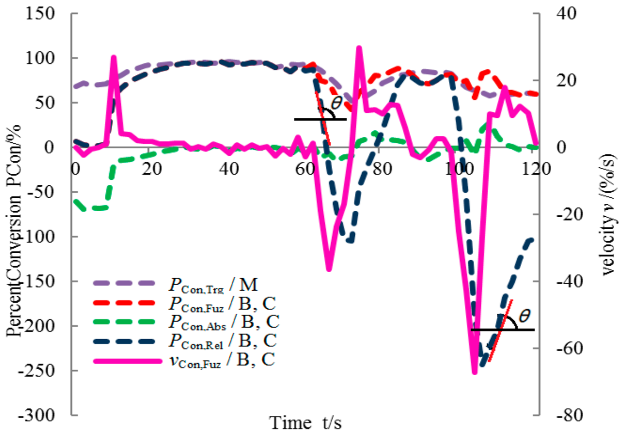

Figure 6. The conversion efficiency tangents.

As a result, between the 30th and 60th second, the NH_3 slip is assumed to be zero thus the UWS needs no correction. Between 60th and 90th or 100th and 120th second, NH_3 slip is severely increased, thus UWS injection should be reduced. Between the 0th and 30th second there is no NH_3 slip, thus UWS compensation be continued. The calculated value and actual experimental value of the NO_x and NH_3 are compared in the low-frequency process. The results are shown in Figure 7.

(1) From the 0 to the 60th second and the 90th to 100th second, the experimental value of the NH_3 concentration downstream from the SCR system is almost 0 ppm. The NO_x concentration and NH_3 concentration calculated by the correction model completely overlap with the experimental values.

(2) From the 60th to 90th second and the 100th to 120th second, there are slight deviations in the hump position between the calculated value and the experimental value of the NH_3 concentration. The two compared values of NO_x concentration no longer completely overlap, but the range and the change rate are apparently the same.

(3) At zero NH_3 slip condition, the calculation deviation of NH_3 concentration was between −10 and 0 ppm and that of the NO_x concentration was between −20 and 20 ppm.

(4) Under high NH_3 slip conditions, the calculation deviation of NH_3 concentration was between −40 and 100 ppm and that of NO_x concentration was between −70 and 70 ppm.

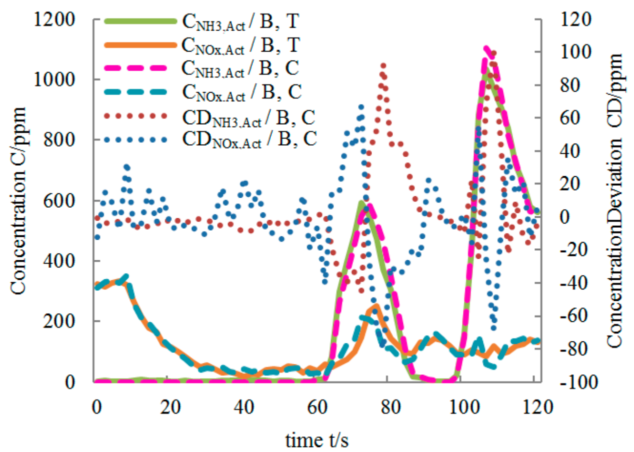

Figure 7. The values and deviations of the NO_x and NH_3 before the correction.

3.2. Low-Frequency Dynamic Process Correction Result

The low-frequency process has been repeated with the dynamic correction of the UWS injection. The NO_x and NH_3 emissions after the correction are shown in Figure 8.

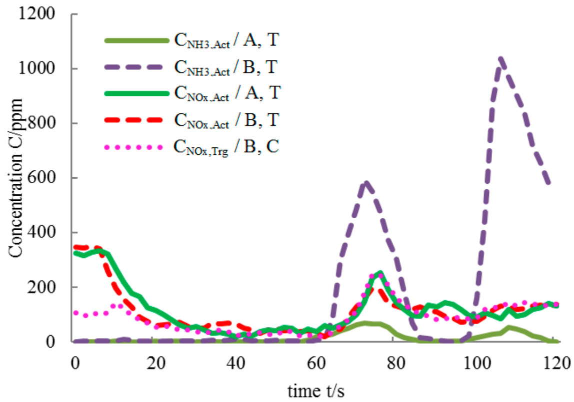

Figure 8. The NO_x and NH_3 emissions before and after the correction.

(1) From the UWS injection starting position to 60th second there was no NH_3 slip. Between the 60th and 120th second the second two humps appeared in the NH_3 concentration curve at less than 80 ppm. That's because of the fractionally unreacted NH_3 slip downstream of the SCR system.

(2) In the low-frequency process, the actual tested value of the NO_x emission was almost the same as the target value. The actual tested value was slightly lower than the target value in the hump region of the NH_3 slip. That's because of the undue UWS injection and more NO_x was restored by the excessive NH_3.

(3) In the hump region of the NH_3 slip, the measured value is slightly higher than the target value of the NO_x concentration. That's because the NO_x sensor was influenced by NH_3 and NO_x at the same time as shown in Equation (7).

Comparing the engine emissions before and after the UWS dynamic correction:

(1) The $C_{NO_x,Act}$ was slightly reduced in the last 60 s on application of the UWS dynamic correction. However, the control method has no significant effect on the value of $C_{NO_x,Act}$ in the low-frequency process.

(2) The $C_{NH_3,Act}$ was also significantly reduced in the last 60 s after the UWS dynamic correction application. The values of $C_{NH_3,Act}$ in the low-frequency process are also greatly influenced by the application of the correction.

(3) Overall, the application of UWS dynamic control method has reduced $\int C_{NH_3,Act}\,dt$ by 92.68%, respectively. Moreover it has also improved $\int C_{NO_x,Act}\,dt$ by 5.58%.

The change trends of the all four kinds of conversion efficiencies are compared after applying the control method as shown in Figure 9.

(1) In the beginning of the low-frequency process, $P_{Con,Abs}$ was smaller than $P_{Con,Trg}$. However, the two curves overlapped after the 15th second.

(2) From 0 to 60th second, $P_{Con,Fuz}$ was the same as $P_{Con,Abs}$, whereas, after the 60th second $P_{Con,Fuz}$ started to deviate with a slightly sinking trend.

(3) Initially $P_{Con,Abs}$ was less than 0 with a rising trend, whereas, it became stable when close to 0 and 15th to 60th second, while from 60th to 120th second it fluctuated many times with an amplitude between −15% and 15%.

(4) $P_{Con,Abs}$ and $P_{Con,Trg}$ were achieved in a shorter period as compared to Figure 4. The sinking amplitude of the $P_{Con,Fuz}$ curve has significantly decreased after the 60th second and became stable in the last 60 s.

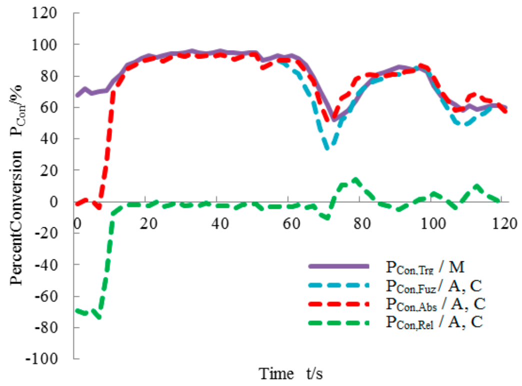

Figure 9. The four kinds of conversion efficiency after the correction.

The calculated values and experimental values of the NO_x and NH_3 were further compared to ensure that the revised data can be well trusted as shown in Figure 10.

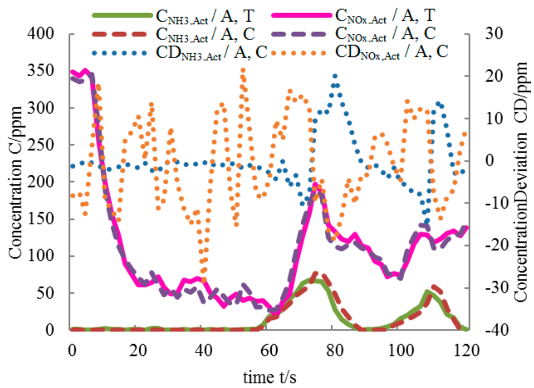

Figure 10. The values and deviations of the NO_x and NH_3 after the correction.

(1) In the corrected low-frequency process the trend of the calculated NH_3 concentration was the same with that of the experimental value. The deviation of the calculation was more obvious in the region of high NH_3 slip as compared to the results shown in Figure 7. The deviation oscillated between −10 to 0 ppm and −5 to 0 ppm with NH_3 slip and between −40 to 100 ppm and −20 to 15 ppm without NH_3 slip.

(2) Moreover, during the corrected low−frequency process trend of the calculated NO_x concentration was the same as the actual tested value. The calculation deviation was uniformly distributed and oscillated between −70 to 70 ppm and −20 to 20 ppm as compared with Figure 7.

(3) NO_x concentration calculation and NH_3 concentration downstream of the SCR system would become more accurate with application of the UWS dynamic correction.

It is compared by the correction factor φ before and after applying the UWS dynamic control method as illustrated in Figure 11 (φ_A and φ_B indicate the correction factors after and before applying the control method, respectively).

(1) From the UWS injection starting to 20th second, φ_B remained at more than 0 with a gradually declining trend. That is for the catalyst NH_3 storage characteristic therefore UWS injection should be compensated.

(2) From 20th to 60th second, φ_B remained constant and close to 0. Now catalyst NH_3 storage has been saturated without NH_3 slip so UWS injection may not be corrected.
(3) From 60th to 120th second, φ_B was less than 0. As compared to Figure 7 it is observed that the change trend of φ_B was contrary to the change trend of NH_3 concentration. It is because of the severely increasing NH_3 slip and UWS injection must be reduced.
(4) φ_A and φ_B were greater than 0 and declined gradually from the starting position of UWS injection till the 20th second. However, the decrease of φ_A was faster than that of φ_B.
(5) φ_A and φ_B remained close to 0 from 20th till the 60th second.
(6) Values of both the factors (φ_A and φ_B) became less than 0 during the last 60 s. Both factors shared two troughs. The trough values of φ_B ranged from −5 to −8 and that of the φ_A was −1 to 0 in curve.

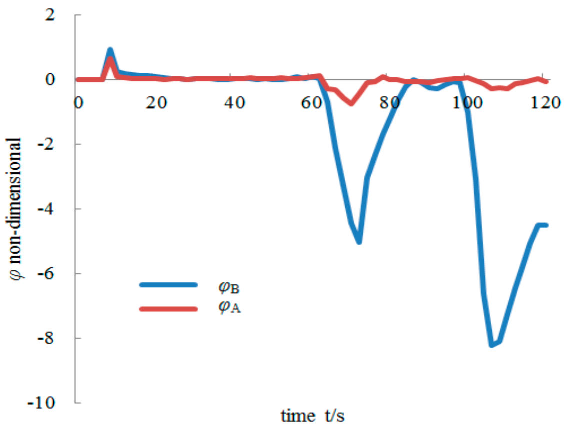

Figure 11. The dynamic correction fact before and after the correction.

The uncertain conversion efficiency $P_{Con,Fuz}$ and its velocity $v_{Con,Fuz}$ before and after applying the UWS dynamic correction are compared as shown in Figure 12:

(1) $P_{Con,Fuz}$ and $v_{Con,Fuz}$ were changed in the last 60 s on applying UWS injection dynamic correction during a high level of NH_3 slip.
(2) The $P_{Con,Fuz}$ after correction appeared more close to $P_{Con,Trg}$ and its range was reduced from −250%–95% to 40%–95% compared to the values before correction.
(3) The range of the $v_{Con,Fuz}$ was reduced from −70%–30% to −10%–10% compared to the value before correction.

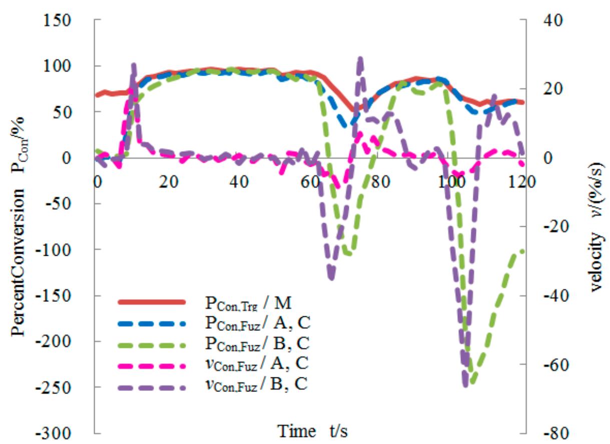

Figure 12. Conversion efficiency and its velocity before and after correction.

3.3. High-Frequency Dynamic Process Correction Result

The emission data comparison in ETC cycle before and after the UWS dynamic control method application is shown in Figure 13.

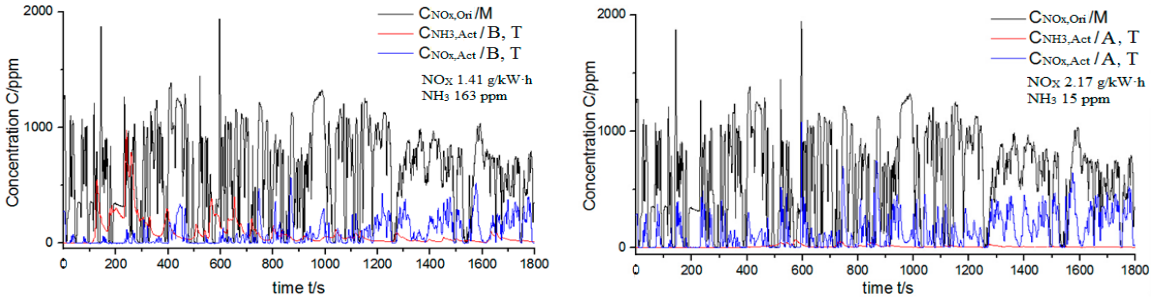

(**a**) (**b**)

Figure 13. Emissions in the engine ETC cycle. (**a**) Before UWS injection dynamic correction; and (**b**) after UWS injection dynamic correction.

The result indicated a great high efficiency of NO_x conversion in the two tests. The NO_x emission was improved by 53.9% and the NH_3 slip was reduced by 90.8% with the application of the control method. The NH_3 slip was also inhibited significantly. The levels of engine NO_x emissions and NH_3 slip were improved and conform to the Euro-V standard.

4. Conclusions

(1) It can be generalized that the "uncertain conversion efficiency curve tangent analysis" method can accurately justify the different NH_3 slip situation.

(2) The calculation deviation can be controlled with NO_x between −20 ppm and 20 ppm and NH_3 between −20 ppm to 15 ppm by application of UWS dynamic correction in a low-frequency process. The NO_x emission was improved by 5.58% and NH_3 slip was reduced by 92.68%.

(3) In the application of UWS dynamic correction in high-frequency process (i.e., during of ETC test), in spite the fact the NO_x emission has been improved by 53.9%, the NH_3 slip was reduced by 90.8%. The level of engine NO_x emissions and NH_3 slip has been improved up to Euro-IV and closer to the Euro-V standard. The newly developed method presents a significant NH_3 slip inhibition.

Author Contributions: Long Li and Wei Lin made the method. Long Li and Wei Lin designed the experiment and organized the entire experiment process. Youtong Zhang made many experimental suggestions and collated the experiment data.

Conflicts of Interest: The authors declare no conflict of interests.

Abbreviations

ASC	Ammonia slip catalysts
ETC	European transient cycle
HCR	High-pressure common rail
PM	Particulate matter
SCR	Select catalyst reduction
UWS	Urea water solution

Symbols

$a_{\mathrm{UWS,Act}}$	Acceleration of $q_{\mathrm{UWS,Act}}$
$C_{\mathrm{N,Act}}$	NO_x concentration measured by the NO_x sensor
$C_{\mathrm{NO}_x\mathrm{,Act}}$	Actual NO_x concentration at the testing position
$C_{\mathrm{NO}_x\mathrm{,Ori}}$	Original NO_x concentration of the engine before aftertreatment
$C_{\mathrm{NO}_x\mathrm{,Trg}}$	The target of NO_x concentration downstream SCR system
$C_{\mathrm{NH_3,Act}}$	Actual NH_3 concentration at the testing position
$C_{\mathrm{DNH_3,Act}}$	Test error of actual NH_3 concentration
$C_{\mathrm{DNO}_x\mathrm{,Act}}$	Test error of actual NO_x concentration
K_{T}	Cross sensitive factor
$P_{\mathrm{Con,Fuz}}$	Uncertain conversion efficiency
$P_{\mathrm{Con,Abs}}$	Absolute conversion efficiency
$P_{\mathrm{Con,Rel}}$	Relative conversion efficiency
$P_{\mathrm{Con,Trg}}$	Targeted conversion efficiency
$q_{\mathrm{UWS,Act}}$	Real-time UWS injection rate after correction
$q_{\mathrm{UWS,Bas}}$	Basic UWS injection rate before correction
$Q_{\mathrm{NO}_x\mathrm{,Red}}$	NO_x conversion potential
$Q_{\mathrm{NO}_x\mathrm{,AcRed}}$	Actual value of the total reduced NO_x
$Q_{\mathrm{NO}_x\mathrm{,TrgRed}}$	Total reduced NO_x under target conversion efficiency
R_{AN}	Ammonia nitrogen ratio set in the SCR control strategy
φ	Correction factor of the UWS injection rate
φ_{A}	Correct factor after applying the control method
φ_{B}	Correct factor before applying the control method Reference

References

1. Johnsont, T.V. Diesel emission control in review. *SAE Int. J. Fuels Lubr.* **2009**, *2*. [CrossRef]
2. Johnsont, T.V. Diesel emissions in review. *SAE Int. J. Eng.* **2011**, *4*, 143–157. [CrossRef]
3. Koebel, M.; Elsener, M.; Kleemann, M. Urea-SCR: A promising technique to reduce NO_x emissions from automotive diesel engines. *Catal. Today* **2000**, *59*, 335–345. [CrossRef]
4. Flynn, P.F.; Hunter, G.L.; Durrett, R.P.; Farrell, L.A.; Akinemi, W.C. Minimum engine flame temperature impacts on diesel and spark-ignition engine NO_x production. *SAE Tech. Pap.* **2000**. [CrossRef]
5. Sharp, C.; Howell, S.; Jobe, J. The effect of biodiesel fuels on transient emissions from modern diesel engines, Part I: Regulated emissions and performance. *SAE Tech. Pap.* **2000**. [CrossRef]
6. Cloudt, R.; Baert, R.; Willems, F.; Vergouwe, M. SCR-only concept for heavy-duty Euro VI applications. *MTZ* **2009**, *70*, 58–63. [CrossRef]
7. Seher, D.; Reichelt, M.; Wickert, S. Control strategy for NO_x—Emission reduction with SCR. *SAE Tech. Pap.* **2003**. [CrossRef]
8. Kammerstetter, H.; Werner, M.; Doell, R.; Kanters, G. The challenge of precise characterizing the Specific large-span flows in urea dosing systems for NO_x reduction. *SAE Tech. Pap.* **2008**. [CrossRef]
9. Kass, M.D.; Thomas, J.F.; Lewis, S.A.; Storey, J.M.; Domingo, N.; Graves, R.L.; Panov, A.; Park, P. Selective catalytic reduction of NO_x emissions from a 5.9 liter diesel engine using ethanol as a reductant. *SAE Tech. Pap.* **2003**. [CrossRef]
10. Chen, C.-T.; Tan, W.-L. Mathematical modeling, optimal design and control of an SCR reactor for NO_x removal. *J. Taiwan. Inst. Chem. Eng.* **2012**, *43*, 409–419. [CrossRef]
11. Nova, I.; Tronconi, E. (Eds.) *Urea-SCR Technology for de NO_x after Treatment of Diesel Exhausts*; Spring: New York, NY, USA, 2014.
12. Shrestha, S.; Harold, M.P.; Kamasamudram, K. Experimental and modeling study of selective ammonia oxidation on multi-functional washcoated monolith catalysts. *Chem. Eng. J.* **2015**, *278*, 24–35. [CrossRef]
13. Opitz, B.; Bendrich, M.; Drochner, A.; Vogel, H.; Hayes, R.E.; Forbes, J.F.; Votsmeier, M. Simulation study of SCR catalysts with individually adjusted ammonia dosing strategies. *Chem. Eng. J.* **2015**, *264*, 936–944. [CrossRef]
14. Feng, T.; Lü, L. The characteristics of ammonia storage and the development of model-based control for diesel engine urea-SCR system. *J. Ind. Eng. Chem.* **2015**, *28*, 97–109. [CrossRef]
15. Rauch, D.; Albrecht, G.; Kubinski, D.; Moos, R. A microwave-based method to monitor the ammonia loading for a vanadia-based SCR catalyst. *Appl. Catal. B* **2015**, *165*, 36–42. [CrossRef]

16. Zhang, H.; Wang, J. Ammonia coverage ratio and input simultaneous estimation in ground vehicle selective catalytic reduction (SCR) systems. *J. Frankl. Inst.* **2015**, *352*, 708–723. [CrossRef]
17. Schär, C.M.; Onder, C.H.; Geering, H.P.; Elsener, M. Control-oriented model of an SCR catalytic converter system. *SAE Tech. Pap.* **2004**. [CrossRef]
18. Willems, F.; Cloudt, R.; van den Eijinden, E.; van Genderen, M.; Verbeek, R.; de Jager, B.; Boomsma, W.; van de Heuvel, I. Is closed-loop SCR control required to meet future emission targets? *SAE Tech. Pap.* **2007**. [CrossRef]
19. Wang, D.Y.; Yao, S.; Shost, M.; Yoo, J.-H.; Cabush, D.; Racine, D.; Cloudt, R.; Willems, F. Ammonia sensor for close-loop SCR control. *SAE Tech. Pap.* **2008**. [CrossRef]
20. Kobayashi, N.; Yamashita, A.; Naito, O.; Setoguchi, T.; Murase, T. Development of simultaneous NO_x/NH_3 sensor in exhaust gas. *Mitsubishi Tech. Rev.* **2001**, *38*, 126–130.
21. Moos, R. A brief overview on automotive exhaust gas sensors based on electroceramics. *Int. J. Appl. Ceram. Technol.* **2005**, *2*, 401–413. [CrossRef]
22. Lu, G.; Diao, Q.; Yin, C.G.; Yang, S.Q.; Guan, Y.Z.; Cheng, X.Y.; Liang, X.S. High performance mixed-potential type NO_x sensor based on stabilized zirонia and oxide electrode. *Solid State Ion.* **2014**, *262*, 292–297. [CrossRef]
23. Jeffrey, W.F. Materials for high temperature electrochemical NO_x gas sensors. *Sens. Actuators B* **2007**, *121*, 652–663.
24. Wang, W. Simulation and Experimental Research on SCR System Control Strategy of Marine Diesel Engine. Master's Thesis, Harbin Engineering University, Harbin, China, 2013.